CHAPTER IV
RESULTS AND DISCUSSION

4.1 Catalyst Preparation

4.1.1 ITQ-21 Synthesis

In ITQ-21 synthesis, many parameters were studied, which are heating method, hydrolyzing time, aging time, and crystallization time. And the suitable condition can be summarized in the following table:

Table 4.1 Suitable conditions for ITQ-21 synthesis

Hydrolyzing time	Aging time	Heating method	Crystallization time
3 days	1 day	hydrothermal	3 days

From the study on the conditions of ITQ-21 synthesis, it can be stated that the most important factor was the hydrolyzing time of the precursors. A shorter period might not be enough for the diffusion and formation of germanium atom, which is considered larger than the conventional atoms (Si and Al), in the framework of zeolite. In ITQ-21 synthesis, started with 16.23 g of sparteine to obtain 1.59 g of ITQ-21 catalyst.

The sample can be identified by XRD, the diffraction data, which were collected at 0.02 (2θ)/step in the range of (2θ), range from 5.00 to 70.00 with a scan speed of 2 s/step, as shown in Figure 4.1.

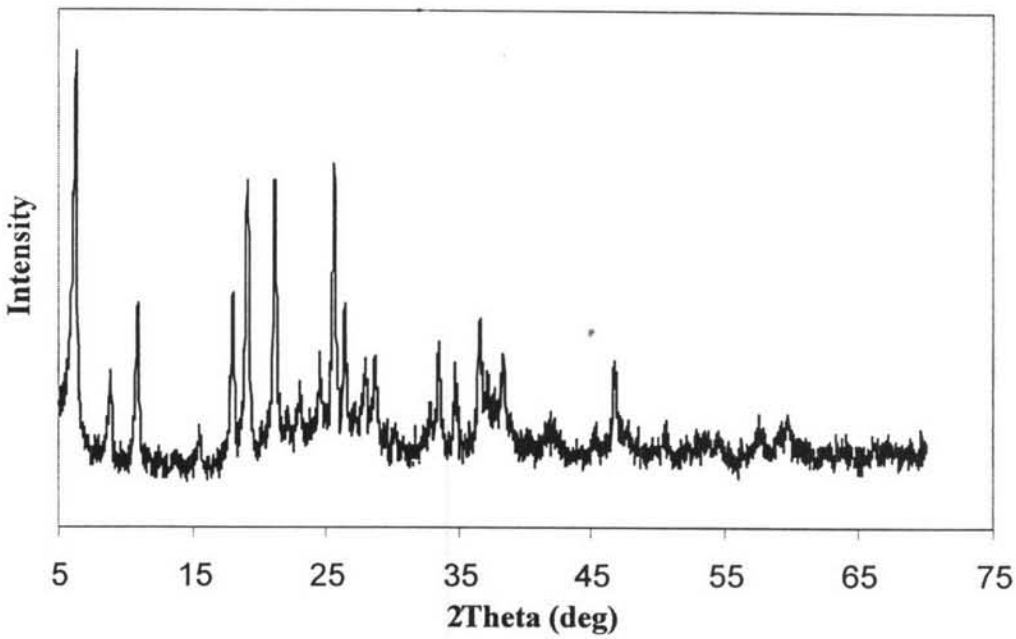

(a)

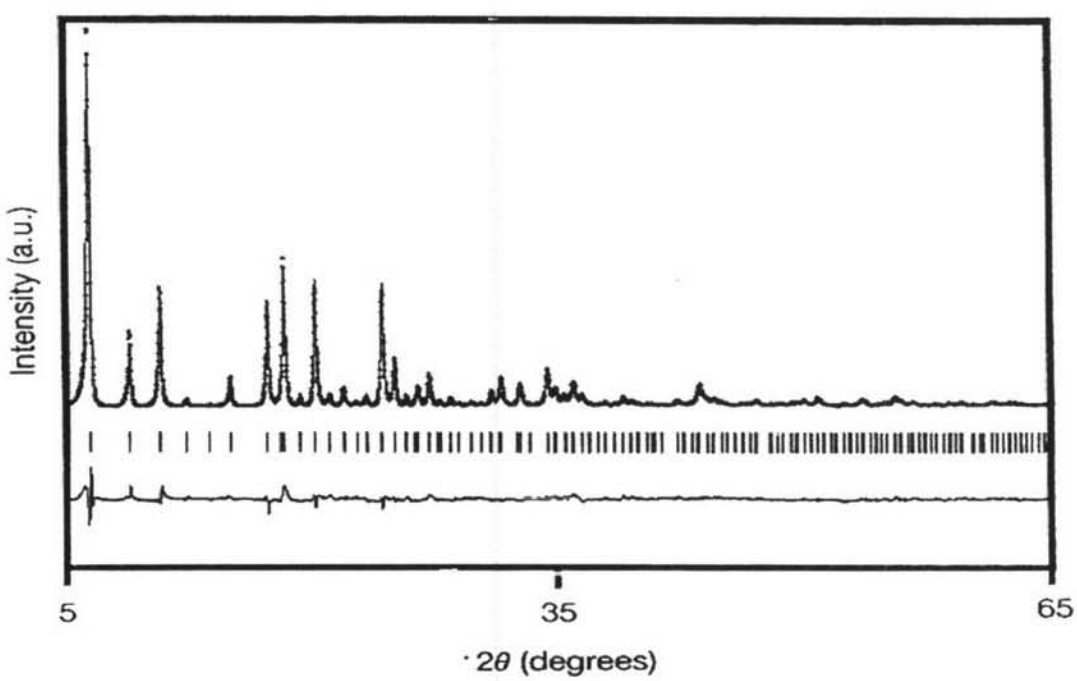

(b)

Figure 4.1 Diffractograms of ITQ-21 obtained from: (a) synthesis using the conditions in Table 4.1, and (b) from the literature (Corma *et al.*, 2002).

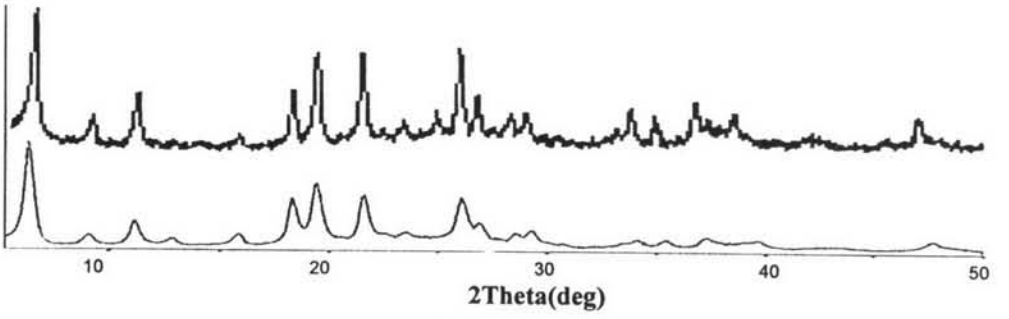

Figure 4.2 XRD pattern of the synthesized ITQ-21 (Top) in comparison with that from the literature (Bottom).

When the diffraction pattern of the synthesized sample is compared with that from the literature, as shown in Figure 4.2, the sample can be identified as ITQ-21, because the peaks between two diffractograms completely match in terms of both peak position and intensity.

4.2 Catalyst Characterization

4.2.1 Scanning Electron Microscope (SEM)

The Scanning Electron Microscope was used to investigate the morphology of the synthesized ITQ-21 catalyst. From Figure 4.3, it is very difficult to identify the shape and size of the zeolite from the SEM micrographs. However, according to Figure 4.3 (b), the zeolite crystals seem to be really small, appearing to be clusters of very small crystallites. Therefore, TEM was employed to visualize these crystallites.

4.2.2 Transmission Electron Microscope (TEM)

The morphology of ITQ-21 can be examined by using Transmission Electron Microscope. From Figure 4.4, it can be indicated that the ITQ-21 is in cubic shape with the crystal size of around 50 to 60 nm.

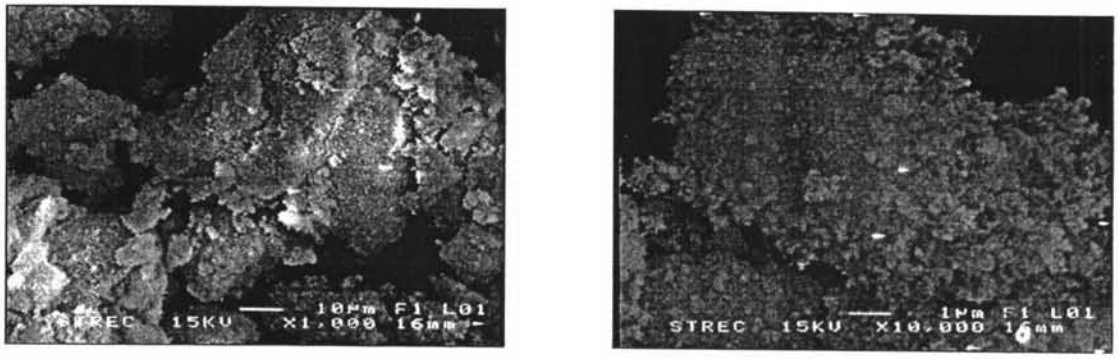

(a) (b)

Figure 4.3 SEM micrographs of ITQ-21 catalyst at different magnifications: (a) 1,000 X, and (b) 10,000 X.

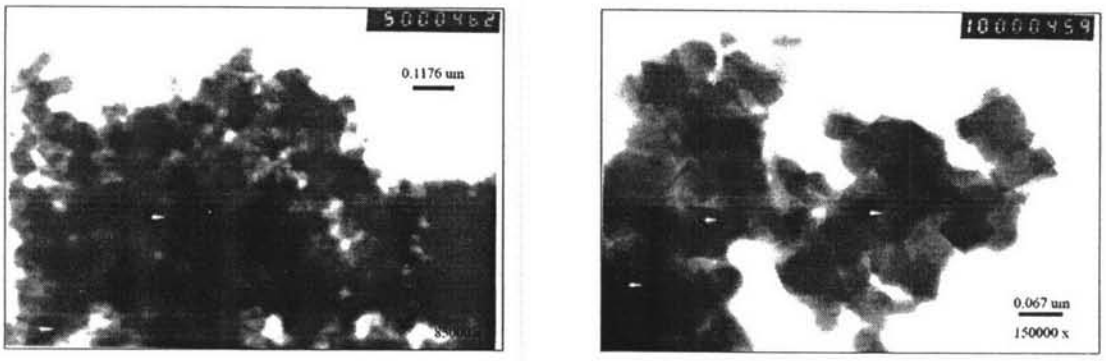

(a) (b)

Figure 4.4 TEM micrographs of ITQ-21 catalyst at different magnifications: (a) 85,000 X, and (b) 150,000 X.

4.2.3 Surface Area Measurement (BET)

The specific surface area, total pore volume and average pore diameter of all prepared catalyst samples were determined by Brunauer-Emmet-Teller (BET) method using Sorpmatic System. N_2 gas was used as the adsorbate at liquid N_2 temperature (-196°C). Samples were treated under He atmosphere at 300°C for 18 hours in order to eliminate volatile adsorbates on the surface before measurements.

By using the BET method, it was found that the synthesized ITQ-21 had specific surface area of around 117 m^2/g and 0.371 cm^3/g of pore specific volume.

4.2.4 Temperature Programmed Desorption of Ammonia (NH_3-TPD)

The Temperature Programmed Desorption of ammonia was performed to measure the acid properties on the surface of catalysts, namely the number of acid sites and the distribution of acid strength.

4.2.4.1 Effect of Metals on Acid Properties

NH_3-TPD profiles for each type of supports are shown in Figure 4.5. Acidity (the area of NH_3 desorption peak) and acid strength (the desorption temperature of NH_3) are plotted in Figures 4.6 and 4.7, respectively.

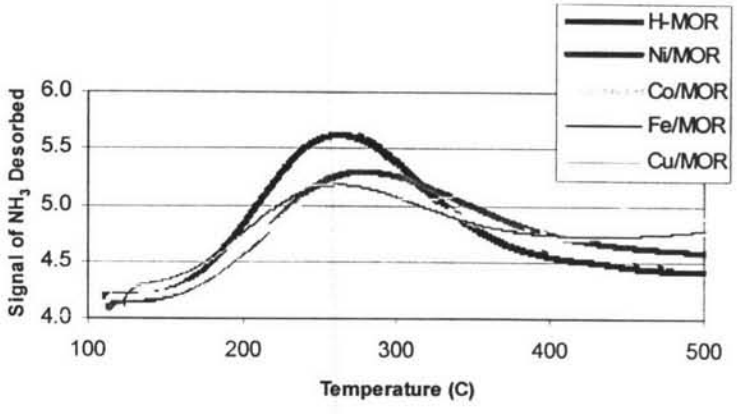

(a)

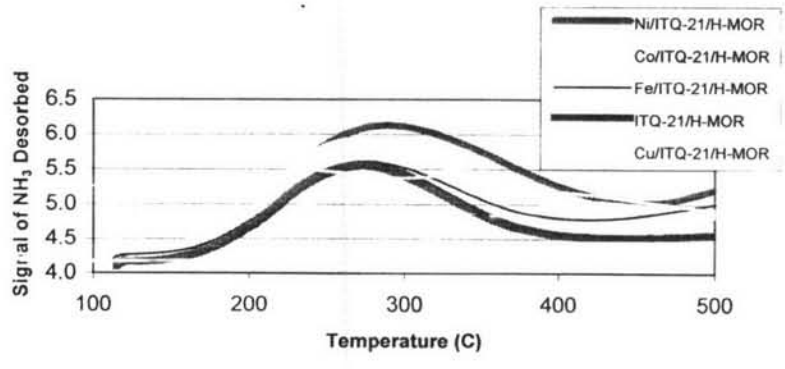

(b)

Figure 4.5 NH_3-TPD profiles of the catalysts with and without metal loading: (a) on the H-MOR support, and (b) on the ITQ-21/H-MOR support.

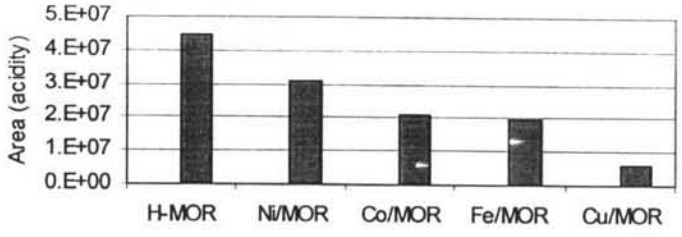

(a)

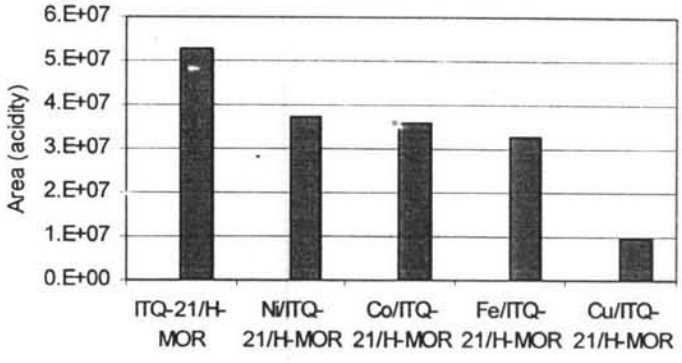

(b)

Figure 4.6 Comparison in acidity of the catalysts with and without metal loading: (a) on the H-MOR support and (b) on the ITQ-21/H-MOR support.

Figure 4.6 shows that the unloaded catalysts (for both H-MOR and ITQ-21/H-MOR) have higher acidity than the metal-containing catalysts, described by the higher NH_3 desorption peak area. Figures 4.6 (a) and (b) show the catalysts loaded on the ITQ-21/H-MOR supports have higher acidity than those loaded on H-MOR alone. Also, it can be seen that the type of metals has the effect on acidity of catalysts. And the metals can be arranged in terms of acidity in the following order: Unloaded > Ni > Co > Fe > Cu. The incorporation of metals possibly caused the reduction of acid sites that can adsorb the probe molecule (NH_3) resulting in the decrease in acidity.

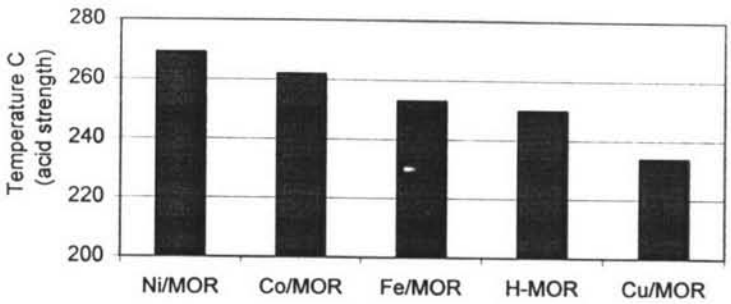

(a)

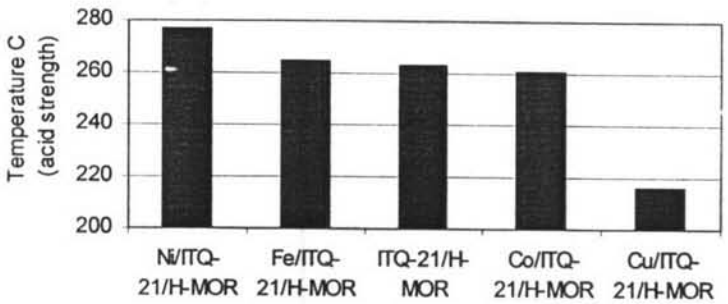

(b)

Figure 4.7 Comparison in acid strength of the catalysts with and without metal loading: (a) on the H-MOR support, and (b) on the ITQ-21/H-MOR support.

Figure 4.7 compares the acid strength of catalysts with and without metal loading on both supports.

For both supports, the unloaded, Fe-loaded, and Co-loaded catalysts have comparable acid strength.

4.2.4.2 Effect of ITQ-21 on Acid Properties

The comparison on the effect of ITQ-21 is shown in Figures 4.8 and 4.9 in terms of acidity and acid strength, respectively.

In Figure 4.8, it is found that mixing of ITQ-21 with H-mordenite as a co-support significantly increases the acidity of all catalysts. Thus, ITQ-21 should have the higher acidity than mordenite zeolite.

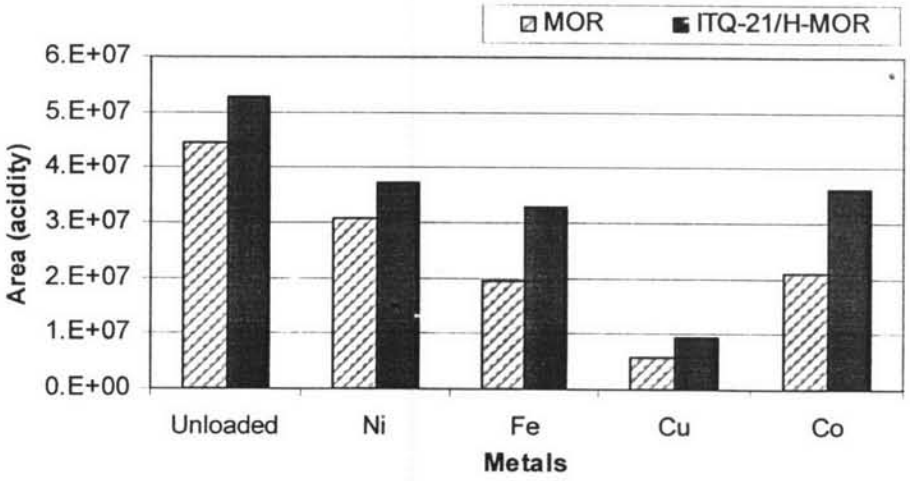

Figure 4.8 Effect of ITQ-21 addition into H-MOR on acidity.

Figure 4.9 shows that mixing of ITQ-21 with H-MOR as a co-support also increases the acid strength of the unloaded catalyst. But, for the metal-loaded catalysts, ITQ-21/H-MOR did not have the clearly effect on acid strength. The difference in acid strength should depend on the type of metals.

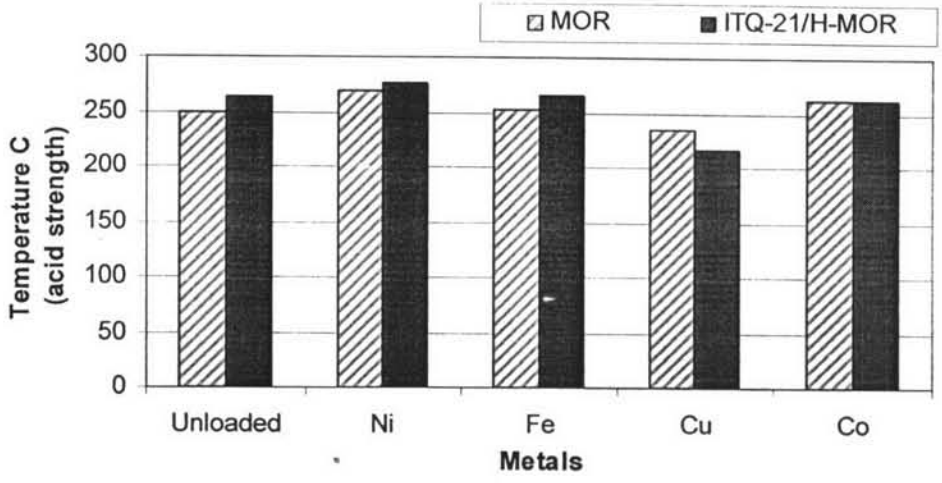

Figure 4.9 Effect of ITQ-21 addition into H-MOR on acid strength.

4.3 Catalytic Activity Measurements

The SCR activity of the catalysts was performed by using the reactant mixture containing 1000 ppm NO, 1000 ppm NH_3, 2% O_2 balanced with helium. The reactant was fed into the reactor with the flow rate of 500 ml/min at the temperature range of 250°C to 400°C. After that, the product effluent was analyzed by a GC and NO_x analyzer.

4.3.1 Effect of The Addition of Metals on SCR Activity

In Figure 4.10, the presence of all metals increases the NO conversion for both types of support. The reason is that metals provided metal sites to adsorb nitrogen oxide and react with oxygen, converting to nitrogen dioxide required for the reactions in the next steps. The absence of metal may need higher reaction temperatures and longer reaction time to complete the reaction (Long, *et al.*, 2002).

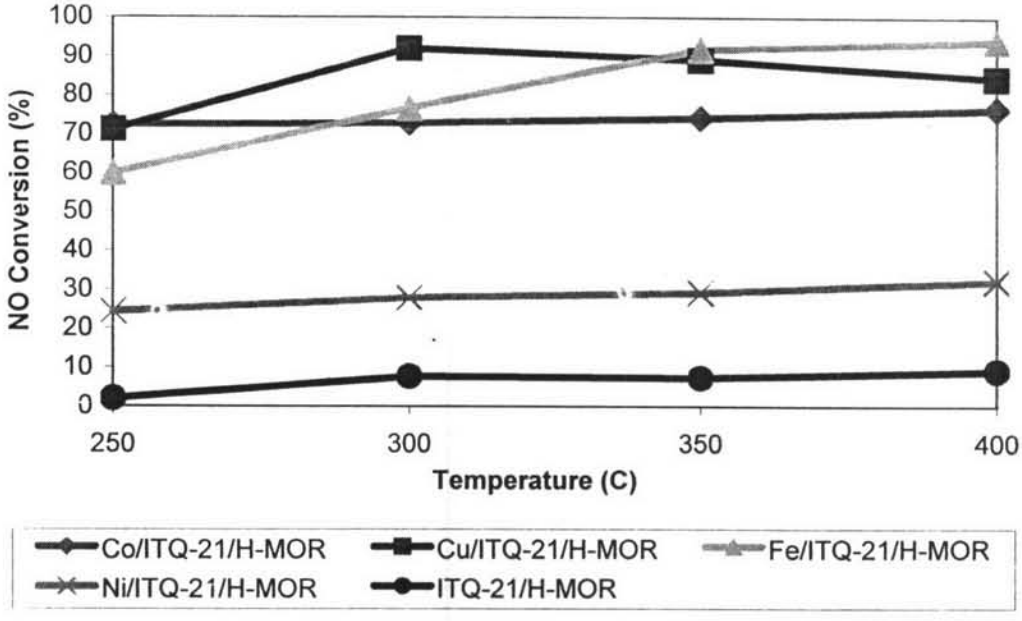

(a)

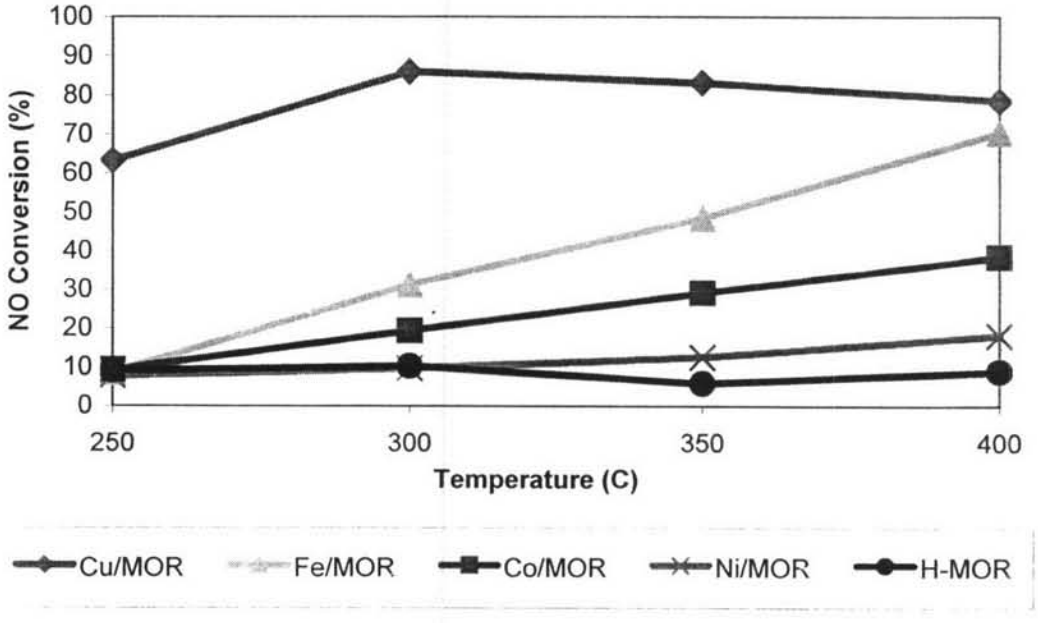

(b)

Figure 4.10 NO conversion of catalysts with and without metal loading: (a) on the ITQ-21/H-MOR support, and (b) on the MOR support.

Figure 4.11 shows the N_2/N_2O selectivity of all catalysts. The addition of metals on catalysts decreases the selectivity because they replace the acid sites of zeolite by metal sites. Furthermore, the presence of metal has more significant effect on reduction of selectivity for the cases of ITQ-21/H-MOR support than those of H-MOR support. Since ITQ-21 has a 3D-pore structure whereas the pores of H-MOR arrange in one-dimension, the metal obstruction in the pores of ITQ-21 can occur more likely than in those of H-MOR.

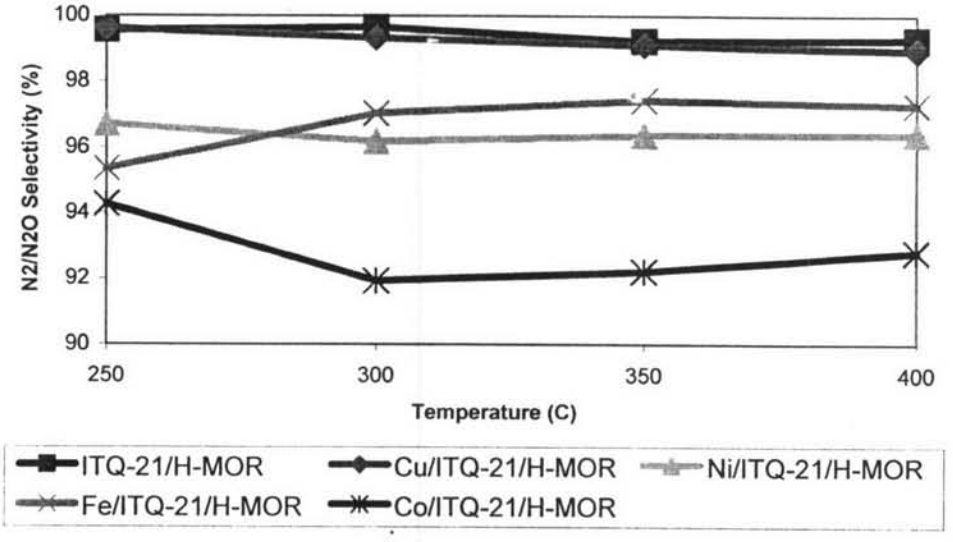

(a)

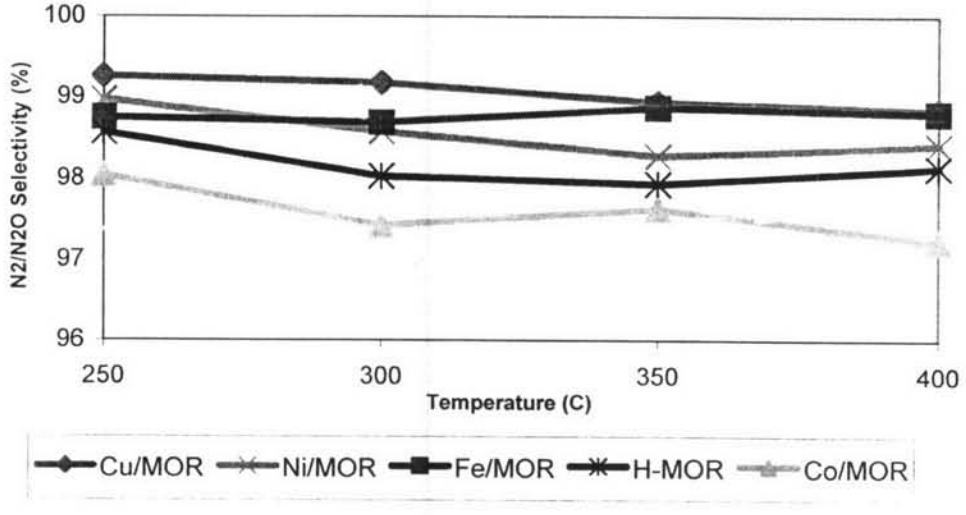

(b)

Figure 4.11 N_2/N_2O selectivity of catalysts with and without metal loading: (a) on the ITQ-21/H-MOR support, and (b) on the MOR support.

4.3.2 Effect of ITQ-21 on SCR Activity

In Figure 4.12, it can be clearly seen that ITQ-21 significantly increases NO conversion of metal-loaded catalysts. The promoting effect of Fe, Co, and Ni on the ITQ-21/H-MOR support is much more pronounce than on the H-MOR support. Copper, on the ITQ-21/H-MOR support, also shows the enhancing effect, but it is not significant because Cu catalysts have already had a high conversion.

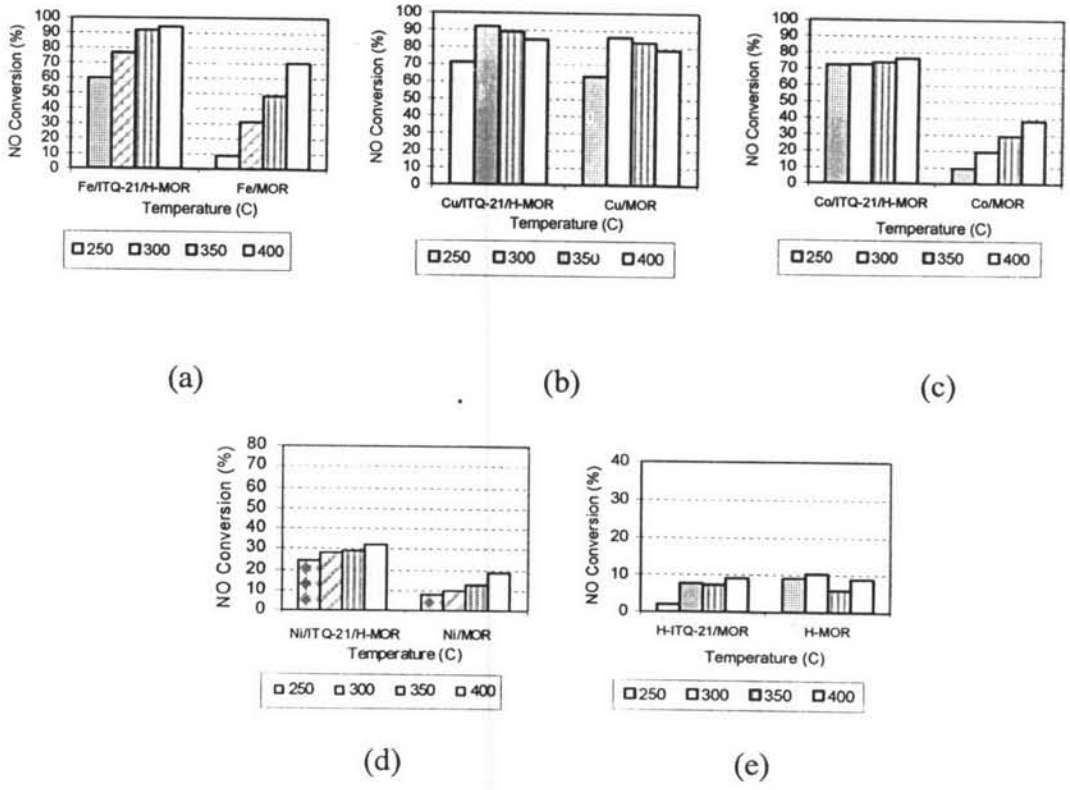

Figure 4.12 NO conversion of (a) Fe-loaded, (b) Cu-loaded, (c) Co-loaded, (d) Ni-loaded, and (e) unloaded catalysts on both H-MOR and ITQ-21/H-MOR supports.

The reason on increasing of NO conversion when ITQ-21/H-MOR was used as the support is that ITQ-21 enhances the acidity of catalysts. This can be confirmed by NH_3-TPD results in Figure 4.8, illustrating the enhancing effect of acidity when using ITQ-21/H-MOR as the support as compared to H-MOR. From Yang, *et al.* (2002), the acid sites of catalyst will adsorb NH_3 to form NH_4^+, which is an important step in NH_3-SCR reaction. Another words, ITQ-21 can provide: (1) three-dimensional pore system to allow fast diffusion of the reactant and intermediate for the reaction, as well as, prevent the blocking of strongly adsorbing species inside

the active pore when compared with the one-dimensional pore system in H-MOR, and (2) higher surface area, to increase more active sites, leading to higher potential to perform the deNO$_x$ reaction.

The ITQ-21/H-MOR support increased the N_2/N_2O selectivity of the unloaded catalysts. It was due to the increase in support acidity. In contrast, the trend of selectivity was unclear in the presence of metals. It might have the combination effect from different types of metal to make the difference in selectivity. The addition of Cu on the ITQ-21/H-MOR co-support increased N_2 selectivity, but the loading of Fe, Co, and Ni on ITQ-21/H-MOR decreased the selectivity. The comparison of N_2 selectivity on different supports is shown in Figure 4.13.

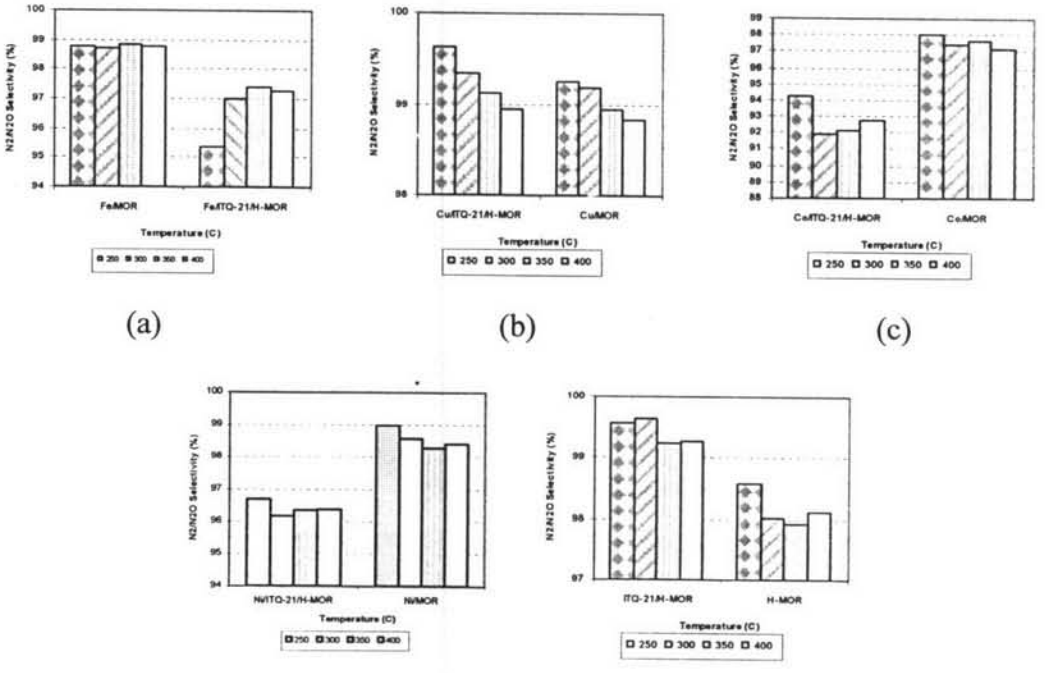

Figure 4.13 N_2/N_2O selectivity of (a) Fe-loaded, (b) Cu-loaded, (c) Co-loaded, (d) Ni-loaded, and (e) unloaded catalysts on both H-MOR and ITQ-21/H-MOR supports.

4.3.3 Effect of Metals on SCR Activity

From Figures 4.14 (a) and (b), it was found that different types of metal showed different NO conversion. In the case of H-MOR support, the copper loaded catalyst expressed the much higher conversion than the others, especially at the lower temperatures. It was the same result as in Choi *et al. (1996)*. Aiso Fe/H-MOR showed high activity at the higher temperatures. On the H-MOR support, the metals can be arranged in term of NO conversion in the following order: Cu > Fe > Co > Ni > Unloaded. That arrangement shows the same tendency as on the ITQ-21/H-MOR co-support, but Fe has the higher NO conversion than Cu at the higher temperatures. On the ITQ-21/H-MOR support, copper, cobalt, and iron gave high conversion at lower temperatures. Cu-ITQ-21/H-MOR reached about 92% NO conversion at 300 °C, whereas Fe-ITQ-21/H-MOR can reach the highest conversion as 94% at 400 °C.

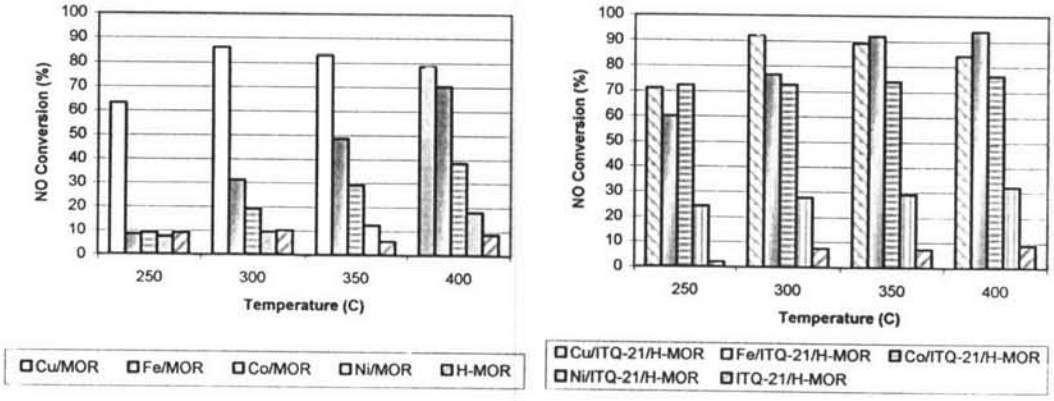

(a) (b)

Figure 4.14 NO conversion on the catalysts promoted with different metals and supports: (a) H-MOR, and (b) ITQ-21/H-MOR support.

In Figure 4.15, N_2/N_2O selectivity of all catalysts was very high. There is no significant effect from different types of metal on the selectivity. The ITQ-21/H-MOR support showed the highest selectivity among all catalysts. This may be resulted from the highest acidity of ITQ-21/H-MOR. But in the H-MOR supported catalysts, they showed the contrast results. They should have had the lower selectivity than the ITQ-21/H-MOR supported catalysts due to the lower acidity, but

they did not. Thus, only acidity should not have the significantly effect on selectivity, metal dispersion and the catalyst structure could also have the essential effect.

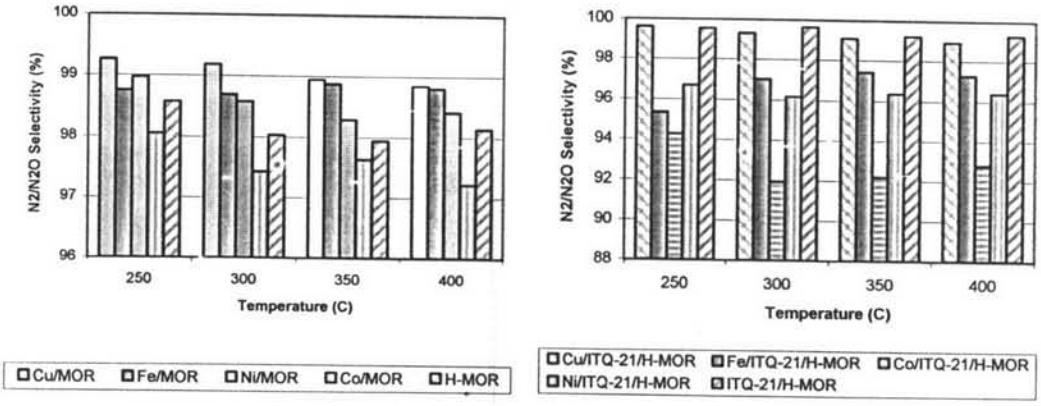

(a) (b)

Figure 4.15 N_2/N_2O selectivity on the catalysts promoted with different metals and supports: (a) H-MOR, and (b) ITQ-21/H-MOR support.

4.3.4 Effect of Reaction Temperature on SCR Activity

Reaction temperature played the important role on NO conversion. Figure 4.16 shows NO conversion of all catalysts at different reaction temperatures. Co-ITQ-21/H-MOR showed the highest conversion at 250°C. At 300°C, Cu-ITQ-21/H-MOR catalyst can reach to 92% NO conversion. At the higher temperature, Fe-ITQ-21/H-MOR can increase the NO conversion to 94% as the highest value among all catalysts.

In general, the higher reaction temperature increases the NO conversion of metal-containing catalysts. And it also depends on the type of metal used to do the reaction.

Figure 4.17 can prove that the reaction temperature do not have the major effect on N_2/N_2O selectivity. Acidity is the mainly parameter affecting the selectivity.

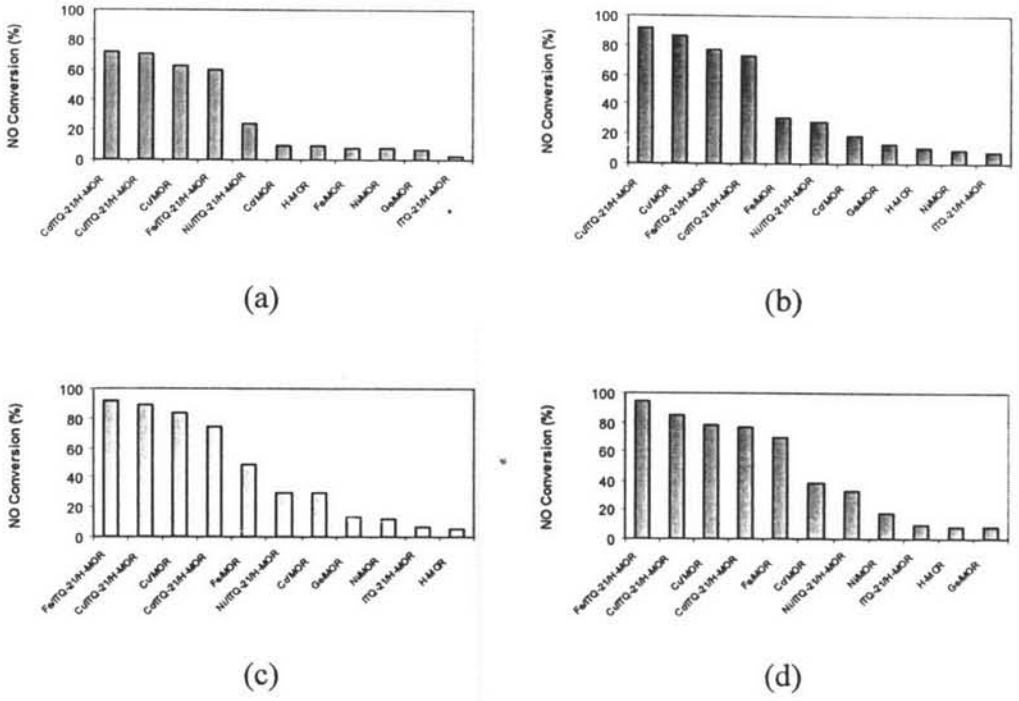

Figure 4.16 NO conversion of all catalysts at different temperatures: (a) 250°C, (b) 300°C, (c) 350 °C, and (d) 400°C.

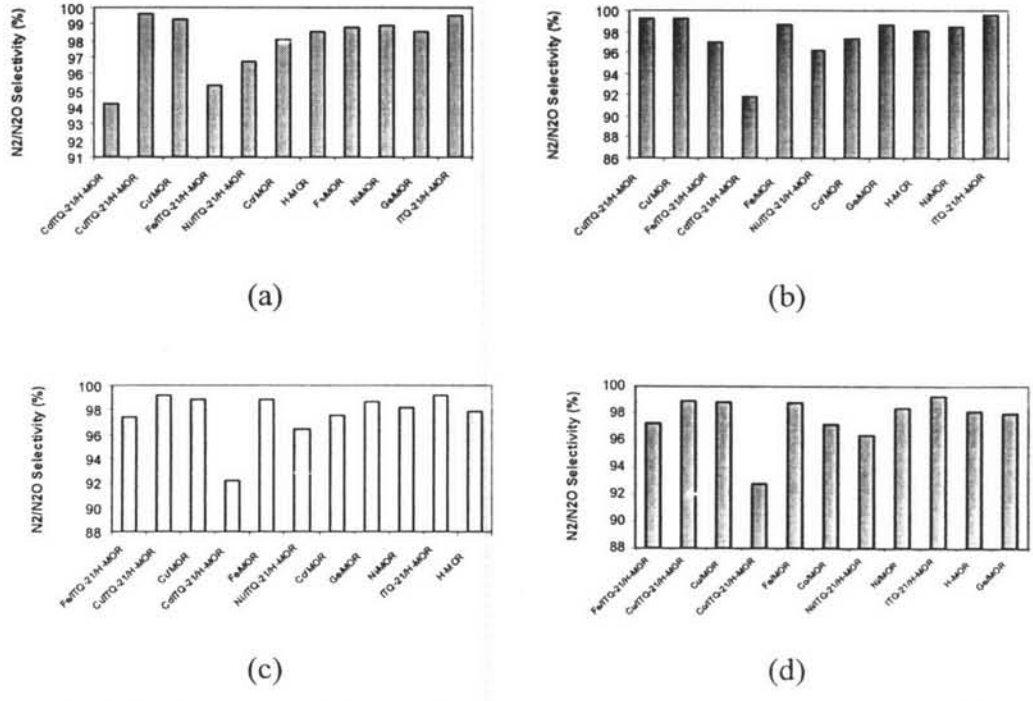

Figure 4.17 N_2/N_2O selectivity of all catalysts at different temperatures: (a) 250°C, (b) 300°C, (c) 350 °C, and (d) 400°C.

4.3.5 Effect of The Presence of Germanium on SCR Activity

Figures 4.18 (a) and 4.19 (a) show that Ge on Ge/MOR can increase the NO conversion in the narrow range of reaction temperature (300-350°C) when compared to the unloaded catalyst (H-MOR). It may provide the metal site to carry on the SCR reaction. However, it can be stated that Ge is still not an appropriate type of SCR metal especially at higher temperatures. Because NO conversion of Ge/MOR is relatively low.

When the activity of germanium between in framework (ITQ-21) is compared with that of Ge in the pore (Ge/MOR), it was found that Ge in the framework can help to stabilize the catalyst as it had the higher NO conversion at the higher temperatures. On the other hand, Ge in the pore of catalyst had the better activity at the lower temperatures.

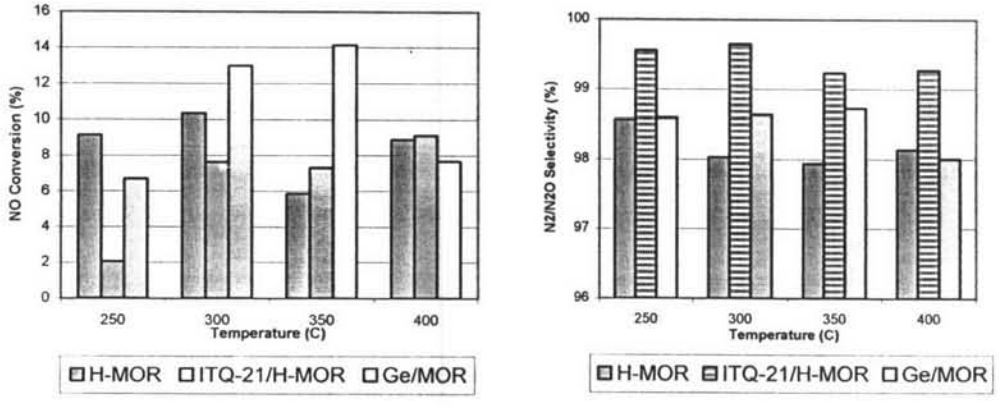

(a) (b)

Figure 4.18 Effect of germanium in the framework on (a) NO conversion, and (b) N_2/N_2O selectivity.

From Figures 4.18 (b) and 4.19 (b), it can be found that there is no effect of germanium on the selectivity of the catalysts. It should mainly depend on acidity of catalysts as discussed on the previous sections.

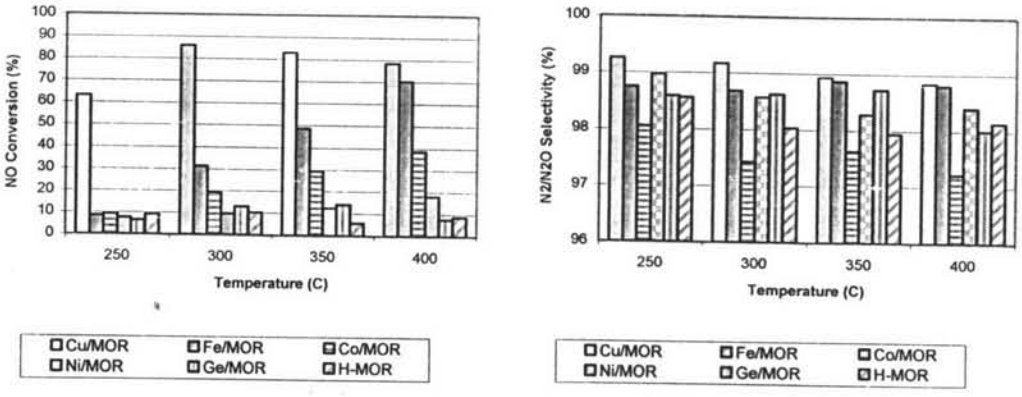

(a) (b)

Figure 4.19 Effect of germanium as a metal on: (a) NO conversion, and (b) N_2/N_2O selectivity.

4.3.6 Reaction Pathways on SCR Activity

The differences in SCR activity with different factors can be explained in term of NO_x reduction mechanism. Figure 4.20 shows the deNO_x mechanism that contains two desired reaction pathways. The first reaction pathway occurs on the acid sites of the catalysts, whereas the second one occurs on the metal sites.

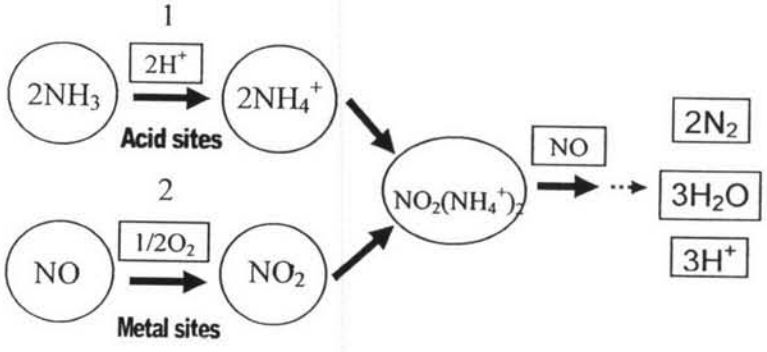

Figure 4.20 NO_x reduction mechanism (Long *et al.*, 2002).

The presence of metals increases NO conversion by enhancing the second reaction pathway, resulting in the higher NO conversion. But, it also produces NO_2, thus, N_2 selectivity will decrease without acid sites on the catalyst.

ITQ-21 increases NO conversion of the metal-containing catalysts. It provides 3D-pore structure enhancing the accessibility of the reactants to the metal

sites, which promotes the second reaction pathway. ITQ-21 also increases N_2 selectivity of the unloaded catalysts due to its acidity that promotes the first reaction pathway.

Germanium in ITQ-21 enhances the first reaction pathway because it increases acidity to the zeolite and then the support. But, germanium in Ge/MOR provides the metal sites that improve NO conversion via the second reaction pathway.